Phase Diagram Structure of the Harper Map

P. Castelo Ferreira[1], F. P. Mancini[1] and M. H. R. Tragtenberg[1,2]

[1] *Department of Physics, University of Oxford, 1 Keble Road, Oxford, OX1 3NP, UK*
[2] *Dep. de Física, Univ. Fed. de Santa Catarina, Florianopólis, SC, Brazil, CEP 88040-900*

We present the phase diagram for the anisotropy parameter λ versus Energy of the Harper map which is equivalent to the semiclassical problem of Bloch electrons in a uniform magnetic field (Azbel-Hofstadter model). We consider rational and irrational values of the magnetic flux ω and give a hierarchical classification of the localized phases relating it to the fractal structure of the diagram. We also present evidence of the existence of an infinite number of Strange Nonchaotic Attractors (SNA) for $\lambda = 1$. [OUTP-00-03S]

Pacs: 03.65.Sq, 05.45.+b, 71.23.Ans Keywords: Harper, Azbel-Hofstadter, Phase Transition, SNA, Fractal

The Schrödinger equation for the Azbel-Hofstadter model [1,2] of Bloch electrons in a uniform magnetic field can be reduce, in the Landau gauge, to the Harper equation [3]

$$\psi_{n+1} + \psi_{n-1} + 2\lambda\cos(2\pi(\phi_0 + \omega n))\psi_n = E\psi_n \quad (1)$$

where ψ_n is the discretized wave function, λ is the ratio between the x and y spacing of the underlying periodic potential and ω is the magnetic flux over one unit cell (see also [4] and [5] and references therein). Under the transformation of variables $x_n = \psi_{n-1}/\psi_n$ we obtain the Harper map [6]

$$x_{n+1} = \frac{-1}{x_n - E + 2\lambda\cos(2\pi\phi_n)} \quad (2)$$

where $\phi_n = (\phi_0 + \omega n) \bmod 1$. We restricted ϕ to the interval $[0, 1]$ since it is just a phase and this restriction does not affect the physical results.

The Lyapunov exponent corresponding to the ϕ dynamics is 0 and the one concerning the x dynamics is given by

$$\bar{y} = \lim_{N\to\infty} \frac{1}{N} \sum_{n=0}^{N} y_n \quad (3)$$

where

$$y_n = \log \frac{\partial x_{n+1}}{\partial x_n} = \log x_{n+1}^2 \quad (4)$$

We obtain numerically the $\lambda \times E$ phase diagram of the Harper map (2) and analyze its structure for rational and irrational values of ω. Our study is based on the analysis of the Lyapunov exponent values in different regions of the map. For the Harper map $\bar{y} \leq 0$. We call the zones with $\bar{y} = 0$ Extended phases (E) and the ones with $\bar{y} < 0$ Localized phases (L). The wave function behavior of the original problem can be recover by reversing the transformation of variables which takes from (1) to (2) obtaining $\psi_n = \psi_0/\prod_i x_i$. For large enough n the wave function behaves as

$$|\psi_n| = e^{\frac{n}{2}\bar{y}}|\psi_0| \quad (5)$$

It is in this sense that we call the phases Localized (ψ has a peak at $n = 0$ and decays exponentially for large n) and Extended (in average ψ has the same amplitude everywhere). For analytical results see [7] and references therein.

We start our analysis of the Harper map from rational values of $\omega = p/q$. Our final aim will be to classify the phase map for irrational ω^* taking as its approximants a succession of rational $\omega_n \to \omega^*$. We choose the inverse of the golden mean $\omega^* = (\sqrt{5} - 1)/2$ which best rational approximants are given by $\omega_n = F_{n-1}/F_n$ where $F_0 = F_1 = 1$ and $F_n = F_{n-1} + F_{n-2}$ is the nth Fibonacci number. Let us first analyze the behavior for $\omega = \omega_n$. All the characteristics discussed are fruit of numerical results. In the $E \times \lambda$ space there are q regions with null Lyapunov exponent corresponding to E phases and $2q+1$ (for even q) or $2q+2$ (for odd q) regions with negative Lyapunov Exponent corresponding to L phases (note that $\bar{y} < 0$ for $E = 0$ and $\lambda > 1$). In these L regions there are q point-like attractors, that is, after a transient period the iterations follow a fixed pattern cycling those q points. ϕ_0 shifts these attractors in ϕ but do not change their x value. Without loss of generality we set $\phi_0 = 0$. As expected the attractors do not depend on x_0 either since $\bar{y} < 0$. The negative Lyapunov value is given by the sum of the q different $\log x^2$ values of the

attractors. At the boundaries between these zones and the zones of zero Lyapunov exponent, corresponding to E phases, the attractors spread and in the limit $N \to \infty$ the x values obeys a *continuous* distribution centered in the previous attractors (see figure 1).

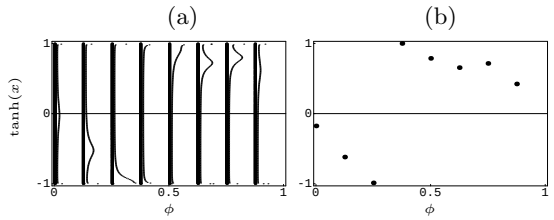

FIG. 1. Transition for rational $\omega = 5/8$ at $E = 0.370773\ldots$ and $\lambda = 0.5$ from Extended (a. $E = 0.34$) to Localized (b. $E = 0.39$) phase. The thin lines in (a) represent densities of iterations.

It is this mechanism that makes the Lyapunov exponent to be 0, the (infinite) net sum of all the $\log x^2$ of the iterations goes to zero. Moving inside the E phases away from the L phases the distributions change in an uniform way until they condense again into new q attractors and we are back in a L zone. These intermediate E zones start as point-like regions at $\lambda = 0$ increasing their width until $\lambda = 1$ and getting narrower for $\lambda \gg 1$ but they never vanish. The boundaries become closer and closer but never meet. Two of such diagrams are pictured in Fig. 2 and 3 for $\omega = 5/8$ and $\omega = 8/13$.

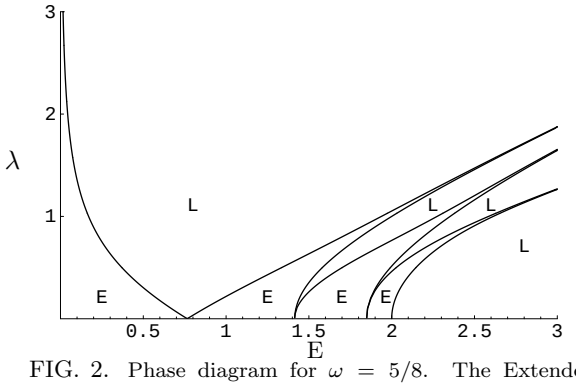

FIG. 2. Phase diagram for $\omega = 5/8$. The Extended phases (E) and the Localized phases (L) are presented. Note that there is an extra line-like L phase at $E = 0$.

The map is symmetric with respect to both axes, we only present the first quadrant. One interesting point is that the ratio of the number of positive over negative attractors is constant in each of the L phases and increases with E. This fact reveals that the phase transitions are due to one of the attractors passing trough the $x = 0$ axis (note that in the w^* limit these ratios become irrationals).

In the $E = 0$ axis something else happens. In this case we will have an E zone starting at $\lambda = 0$ and ending before $\lambda = 1$ (for even q) or at $\lambda = 1$ (for odd q). This zone divides into two distinct regions. The first starts at $\lambda = 0$ where there are q (for even q) or $2q$ (for odd q) attractors. Exactly half of them correspond to positive values of x and the other one to negative distributed in such a way that $\bar{y} = 0$. In the second region these attractors spread giving rise to continuous distributions, the Lyapunov exponent remaining null. Increasing λ the distributions condensate again and in the remaining of the $E = 0$ axis we return to *normality*. That is, the Lyapunov exponent becomes negative and there are q attractors. The length of the second region of the E zone, where the attractors spread, decreases with q. In this case for different values of ϕ_0 the point-like attractors are scramble in the $x \times \phi$ space (not just shifted) but the value of the Lyapunov exponent does not change and neither does the E/L properties of the zone.

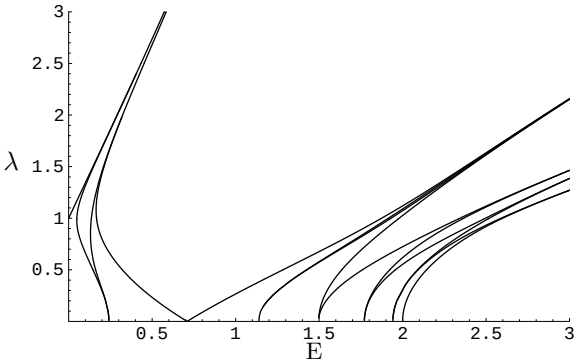

FIG. 3. Phase diagram for $\omega = 8/13$.

Returning to the global picture, if we increase n the E zones split and new thinner L zones emerge (see Fig. 3 as compared with Fig. 2). Note that in the irrational limit ω^* the point-like attractors in the L phases become a line due to the ergodicity of ϕ. In this limit the number of these zones become infinite. The phase transition lines become denser and denser and they eventually cross at the critical value $\lambda = 1$. The Lyapunov exponents go to zero at these points of intersection which become the ends of the lines. Then an infinite number of point-like phase transitions (similar to the usual critical points) emerge. Figure 4 illustrates this process by showing the Lyapunov exponents at $\lambda = 1$ for suc-

cessive values of ω_n. The $\phi \times x$ diagram at these infinite many points that emerge at $\lambda = 1$ are SNAs as the one pictured in figure 5 (c).

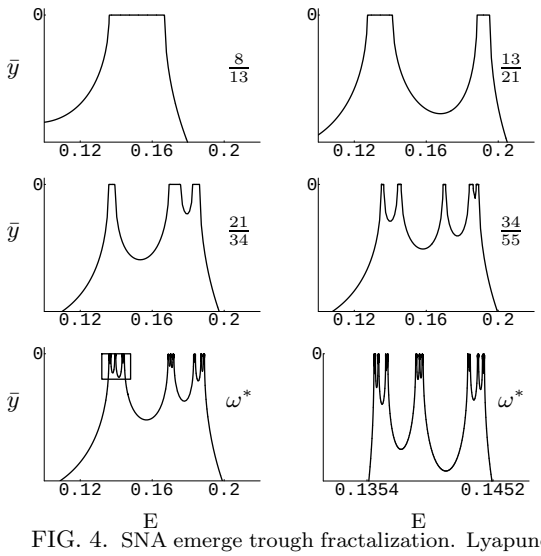

FIG. 4. SNA emerge trough fractalization. Lyapunov exponents for $\lambda = 1$: Top four plots, $\omega_n = F_n$ $(n = 6, 7, 8, 9)$; Two bottom plots, irrational $\omega = \omega^*$.

For $E = 0$ the first region of the E zone, where we have point-like attractors (starting at $\lambda = 0$) increases with n. In the limit $\omega \to \omega^*$ The second region condenses precisely at $\lambda = 1$. It is this the mechanism that generates an SNA at $E = 0$ and $\lambda = 1$. (see [8] and references therein for further explanation of this particular case).

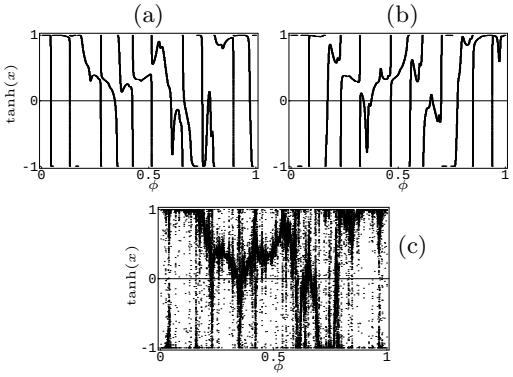

FIG. 5. Maps for ω^* and $\lambda = 1$ at $E = 2.342$ (a), $E = 2.347$ (b) and $E = 2.3447775\ldots$ (c). In (a) we have $\eta = 11$, in (b) $\eta = 10$ and (c) is a SNA.

The phase diagram becomes in the limit of irrational ω^* a fractal (see Fig. 6 and 4), more exactly, a Cantor set [9]. Note that for $\lambda > 1$ the Lyapunov exponents become always negative although they maintain their *bumpy* structure (see Fig. 4). This means that the transition between different L phases is smooth without undergoing an E phase.

We proceed to classify the zones corresponding to localized phases constituting that fractal. We take as label of our classification η, the number of times the successive iterations (ϕ is the ordering referring to successive) undergoes a jump from $x = +\infty$ to $x = -\infty$. This classification can be better understood in the limit of irrational ω^*. Take a map from the space $x \times \phi$ to a torus such that we consider the identifications $0 \cong 1$ for ϕ and $+\infty \cong -\infty$ for x. This can be though as imposing periodic boundary conditions on the coordinates. Now the line attractors are living on the surface of a torus and η is nothing else than the winding number of the line attractors in the x axis. Note that the winding number in the ϕ direction is always 1. Again for $E = 0$ and $\lambda < 1$ the scenario is different from the rest of the diagram: we have two lines with winding number 0 in the x axis and 1 in the ϕ axis.

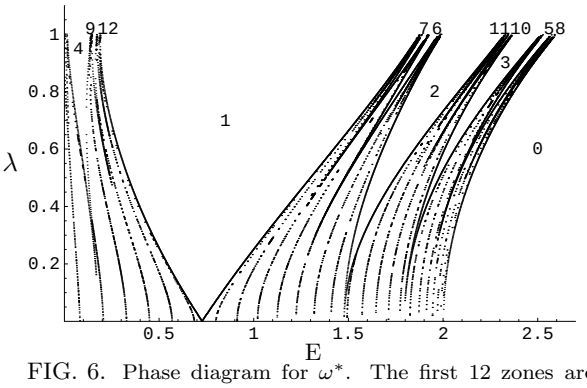

FIG. 6. Phase diagram for ω^*. The first 12 zones are labeled in the diagram.

The great advantage of the hierarchy and labels of this classification is that it coincides with the ordering of the areas occupied by the corresponding phases. The diagram for irrational ω^* and the classification of areas up to $\eta = 12$ is presented in Fig. 6. The attractors for $\eta = 10$ and $\eta = 11$ are presented in Fig. 5 (a) and (b). Let us define the generic rules to build the classification tree. First note that the Localized zone on the far right (for $E > 2$) has always $\eta = 0$ and the Lyapunov exponent decreases with the energy. For each of the ω_n the next zone to the left is always labeled with an element of the Fibonacci succession $\eta = F_{n'}$ for some $n' \leq n$. We choose to organize our classification in horizontal levels. The last label in the right at level n' is given

by $F_{n'}$ (see Fig. 7). In every level there are exactly $F_{n'-2}$ labels such that $F_{n'-1} < \eta_{\text{level } n'} \leq F_{n'}$. We obtain a triangular structure with $\eta = 1$ in the top vertex and the $\eta^*_{n'} = F_{n'}$ distributed in sequence in the right edge. In the left edge the n' levels are filled only for $n' = 3n'' + 1$ (for every n'') with labels $\eta = F_{3n''} + F_{3n''-2}$. We just described the structure of the edges, we need now to fill the triangle. Take the triangle completely built up to level m and let us construct the next $m + 1$ level. Call the first element in the bottom right vertex (at level m) $\eta^*_m = F_m$. Now group the labels on the edges of the triangle already built in pairs starting from η^*_m and excluding any eventual element of level m lying in the left edge. The elements of the first pair (to which η^*_m belongs) are summed together to give the label $\eta^*_{m+1} = F_{m+1}$ to be placed in the right edge of the next level. We take then η^*_m and sum it to the elements of the remaining pairs. The resulting elements will be placed in the new level $m + 1$ between the original pair that was used to generate them. If up to that level there are no labels between the original pair (we mean between the two vertical lines starting in the elements of the original pair) we swap them, otherwise they are placed after the left (before the right) original generators and before (after) other eventual labels that exist in between the original generators. Note that in this way we are always generating new pairs of labels in the bulk of the triangle. After finishing the pairs in the edges we proceed to sum η^*_m to the remaining bulk pairs of level $m' < m$ only and applying the previous rules. Note that the bulk pairs at level m will be only used to generate new pairs for level $m'' > m+1$. It is remaining one final check, from 3 in 3 levels will happen (due to the structure of the Fibonacci succession-even, odd, odd) that we cannot group the labels in the edges in pairs because their are in odd number. In that case we take the last element in the left edge (bottom) which have been left alone (it will be $\eta = F_{m-3} + F_{m-5}$) and sum to it η^*_m placing it at the left edge of the level $m+1$ we are building. In this way we build the previously mentioned structure for the left edge. The triangular hierarchy is pictured in figure 7, see also figure 6 to compare the corresponding phases in the diagram.

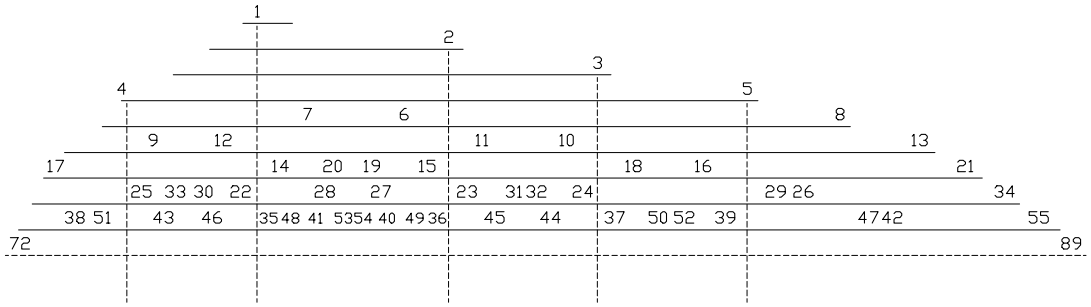

FIG. 7. Hierarchy tree of the fractal structure. Compare with the diagram of figure 6.

In this paper we have described the phenomenology of strange nonchaotic dynamics in the quasiperiodically driven Harper map. We have analyzed the occurrence of SNAs in the full range of the Energy and have proposed a mechanism through which SNAs are created in this system at $\lambda = 1$. By successive approximations we have built the $E \times \lambda$ phase diagram for irrational $\omega^* = (\sqrt{5} - 1)/2$, analyzed it and classified its many infinite Localized phases.

The work of PCF is supported by PRAXIS XXI/BD/11461/97 grant from FCT (Portugal). The work of FPM is supported by EPRSC studentship 97304299 and by Fondazione A. Della Riccia. The work of MT is supported partially by FINEP/Brazil.

[1] M. Ya Azbel, Sov. Phys. JETP **19**,634 (1964).
[2] D. R. Hofstadter, Phys. Rev. **B14**, 2239 (1976).
[3] P. G. Harper, Proc. Phys. Soc. London **A68**, 874 (1955).
[4] E. Brown, Phys. Rev. **133**, 1038 (1963).
[5] A. G. Abanov, J. C. Talstra and P. B. Wiegmann, Nucl. Phys. **B525**[FS], 571 (1998).
[6] J. A. Ketoja and I. I. Satija, Physica **D109**, 70 (1997).
[7] S. Y. Jitomirskaya and Y Last, Commun. Math. Phys. **195**, 1 (1998).
[8] A. Prasad, R. Ramaswamy, I. I. Satija and N. Shah, Phys. Rev. Lett. **83**, 4530 (1999).

[9] J. Bellisard and B. Simon, J. Funct. Anal. **48**, 408 (1982).